

Article

Enhancing Vibration Control in Cable–Tip–Mass Systems Using Asymmetric Peak Detector Boundary Control

Leonardo Acho [†]  and Gisela Pujol-Vázquez ^{*,†} 

Department of Mathematics, Universitat Politècnica de Catalunya-BarcelonaTech (ESEIAAT),
08222 Terrassa, Spain; leonardo.acho@upc.edu

* Correspondence: gisela.pujol@upc.edu; Tel.: +34-9373-98159

† These authors contributed equally to this work.

Abstract: In this study, a boundary controller based on a peak detector system has been designed to reduce vibrations in the cable–tip–mass system. The control procedure is built upon a recent modification of the controller, incorporating a non-symmetric peak detector mechanism to enhance the robustness of the control design. The crucial element lies in the identification of peaks within the boundary input signal, which are then utilized to formulate the control law. Its mathematical representation relies on just two tunable parameters. Numerical experiments have been conducted to assess the performance of this novel approach, demonstrating superior efficacy compared to the boundary damper control, which has been included for comparative purposes.

Keywords: boundary control; flexible cable; partial differential equation; control design; peak detector model

1. Introduction

In numerous industrial applications, systems are often represented by partial differential equations (PDEs), where the targeted physical quantity relies on both position and time, as noted by Morris [1]. There are two primary PDE control settings depending on the nature of control actuation; it can either be distributed throughout the system's domain, or the actuation and sensing are confined solely to the boundary conditions [2–5]. Boundary control is regarded as more physically realistic due to the non-intrusive nature of the actuation and sensing, as emphasized by Kao and Stark [6]. In fact, the design of boundary control for cable-based systems presents a significant challenge and finds relevance in various control engineering applications, such as floating platforms for offshore wind turbines [7,8], overhead cranes equipped with flexible cable mechanisms [9–11], conveyor belt devices [12], oil-drilling actuators [13], and so on [14–22]. See Figures 1 and 2 for examples of these applications.

These applications are prominent due to the favorable attributes of cables, such as their relatively low weight, flexibility, strength, and ease of storage, as noted by de Oliveira and Cajueiro [23]. However, if the induced vibrations are not effectively filtered out in the cable system, they can significantly deteriorate system performance and eventually lead to critical failures. In the existing literature, various control strategies have been proposed to address this issue. Therefore, boundary vibration control remains a crucial area of focus in these applications. For an in-depth review on this topic, see Zhao et al. [21] and the references therein. To achieve a state-of-the-art understanding of vibration control applied to cable mechanical systems, the cable–tip–mass model serves as a reference challenge. Additionally, in [24], the author reduce riser vibration through stochastic control methods, while Zou et al. [25] present an adaptive control system with backlash. Furthermore, Koshal et al. [26] and Zhang et al. [27] propose an observer-based boundary control approach, as in [28]. In [29], the authors present an active disturbance rejection controller, where the energy system converges to equilibrium with an exponential manner. Adaptive control



Citation: Acho, L.; Pujol-Vázquez, G. Enhancing Vibration Control in Cable–Tip–Mass Systems Using Asymmetric Peak Detector Boundary Control. *Actuators* **2023**, *12*, 463. <https://doi.org/10.3390/act12120463>

Academic Editor: Guang-Hong Yang

Received: 16 November 2023

Revised: 29 November 2023

Accepted: 6 December 2023

Published: 11 December 2023



Copyright: © 2023 by the authors. Licensee MDPI, Basel, Switzerland. This article is an open access article distributed under the terms and conditions of the Creative Commons Attribution (CC BY) license (<https://creativecommons.org/licenses/by/4.0/>).

methods, as described in [30], are applied, but despite not relying on the measurement or estimation of system states, the energy consumption is found to be excessive.

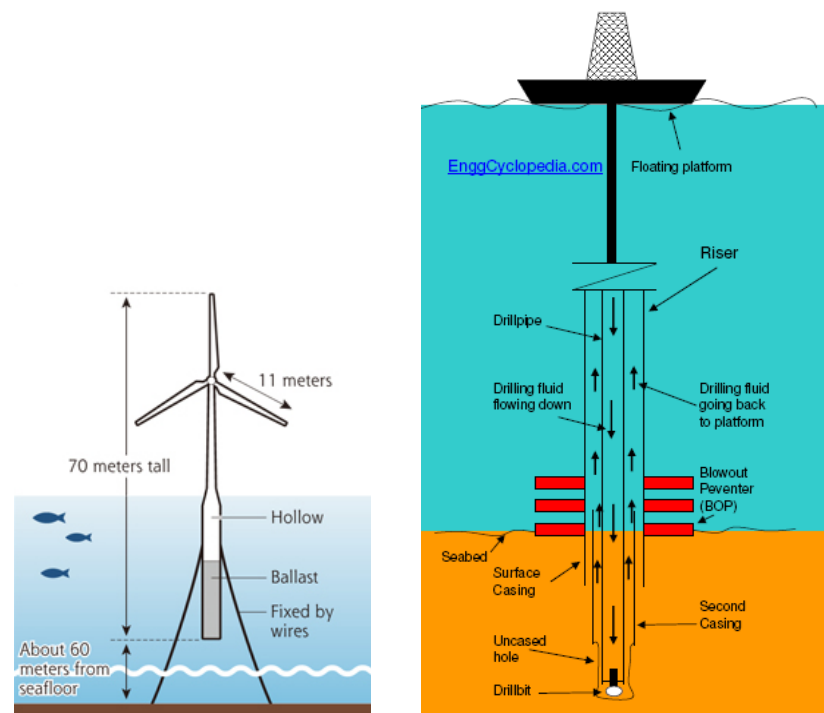


Figure 1. Floating platform for offshore wind turbines (cleantechnica.com); oil-drilling actuators (EnggCyclopedia.com).

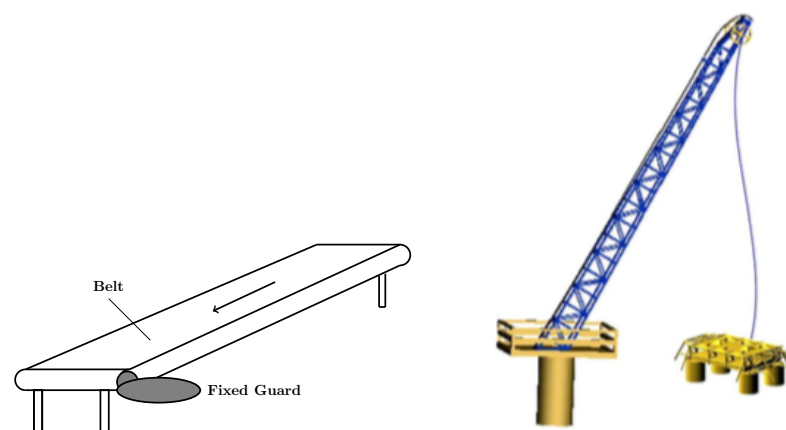


Figure 2. Conveyor belt device (scheme); overhead crane with flexible cable mechanisms.

Moreover, the application of the asymmetric peak detector mechanism has demonstrated its utility in reducing vibrations in flexible structures, as highlighted in Pujol's work [31]. The conventional peak detector system identifies peak values within the input signal, as mentioned by Meng [32]. The current modification introduces two parameters to regulate the behavior of the input signal, resulting in the development of a non-symmetric controller configuration. The primary goal is to derive a modified control input that enhances vibration attenuation. We implement this approach for a cable–tip–mass system, considering a modification of a standard boundary controller for comparative analysis. According to numerical experiments, the performance of this modified approach surpasses that of the damper controller case [23,33,34]. Specifically, we effectively adapt the peak detector algorithm to our boundary control design for attenuating vibrations along the cable or string in our mechanical cable–tip–mass device. Additionally, we provide a formal

proof of this assertion using Lyapunov theory. This paper represents an enhanced version of our prior work presented in [5]. The primary contribution of this paper lies in validating a seemingly unrelated technique, such as the peak detector model, when applied to the cable–tip–mass system. This paper offers several key contributions:

- Introduction of a boundary strategy centered on detecting peak vibration values and subsequent proof of its bounded-input bounded-output (BIBO) stability.
- Proposal of two design parameters aimed at enhancing the flexibility of peak detection. Their values can be determined using specific performance indices.
- Conducting simulations that compare the performance of this approach with a classic boundary controller, demonstrating its efficacy.

Furthermore, the practical implementation of the control algorithm presents a considerable challenge in technological progress. Reference [35] provides a detailed account of particular mechanical configurations within the mechatronic stiffness concept, offering insights into its traits, behavior, and the achieved control outcomes.

The remaining sections of the paper are organized as follows. Section 2 outlines the mathematical model of the cable–tip–mass system employed for our purposes, along with the pertinent assumptions relevant to real-world applications. It also introduces the novel asymmetric peak detector model, with its stability established in terms of Lyapunov theory. Section 3 comprises several numerical simulations that demonstrate the effectiveness of the proposed control design, discussed in Section 4. Finally, Section 5 presents the key conclusions derived from this study.

2. Materials and Methods

2.1. Cable–Tip–Mass System

The system illustrated in Figure 3 depicts the boundary-actuated cable–tip–mass system, which can be mathematically represented by [23]:

$$\rho u_{tt}(x, t) - T_0 u_{xx}(x, t) = 0, \quad (1)$$

$$u(0, t) = 0, \quad t \geq 0, \quad (2)$$

$$m u_{tt}(L, t) + T_0 u_x(L, t) = f(t), \quad t \geq 0, \quad (3)$$

where ρ denotes the mass per unit length of the cable, m is the mass of the actuator located at the free boundary space, T_0 is the applied tension to the cable, L is the cable length, and $x \in [0, L]$ represents the independent position variable. Variable $u(x, t)$ represents the transverse position at the x -position for a t -time, and $f(t)$ denotes the boundary control force. Finally, with regards to notation, the provided subscripts denote the corresponding partial derivatives, as is customary [23]. To establish a practical control framework, two assumptions must be introduced [21]:

- The amplitude of $u(x, t)$ is very small.
- T_0 is constant all along the cable.

In summary, the aim of the boundary control is to determine a controller $f(t)$ that decreases the intensity of cable vibrations. It can be stated in terms of bounded-input bounded-output (BIBO) stability; $|u(x, t)| \in L_\infty$ if $f(t)$ is bounded too. To conclude this section, we observe that the open-loop response (with $f(t) = 0$) of this system is undamped.

The implementation of the control algorithm, schematically represented in Figure 3, is a challenging issue of technological development. Reference [35] describes selected mechanical arrangement of the mechatronic stiffness concept, its features, behavior, and control results.

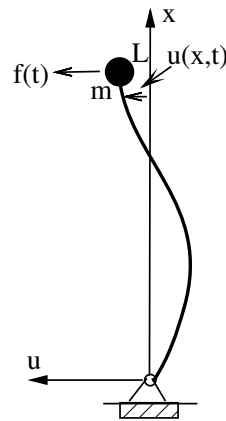


Figure 3. A simplified cable–tip–mass system, with local coordinates and boundary conditions. One end of the string is pinned while the other end is linked to an actuator $f(t)$. Our assumption accounts for uniform tension along the entire length of the string.

2.2. Asymmetric Peak Detector Model

In electronics [32], a peak detector system is applied to estimate the peak voltage value of a given signal. In this section, we present the mathematical model of the asymmetric peak detector system, proving its BIBO stability.

2.2.1. Definition and Characterization

Essentially, a standard peak detector system is implemented by utilizing a diode (D), a capacitor (C), and a resistor (R), as depicted in Figure 4. In this configuration, the input signal $v_i(t)$ is fed into the peak detector system, and subsequently, the output signal $y(t)$ provides an estimate of the peak voltage value of $v_i(t)$. The retention duration for storing the peak value of $v_i(t)$ in the capacitor is regulated by the specific values of R and C.

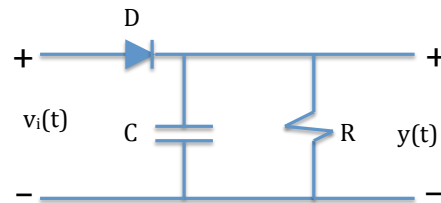


Figure 4. Simplified electronic circuit of the peak detector system. $y(t)$ displays the peak information on the input signal $v_i(t)$. The memory time to keep the peak value of $v_i(t)$ stored in the capacitor is controlled through the values of R and C.

By applying Kirchhoff laws to the electronic circuit, we derive the differential equation governing this system:

$$\dot{y}(t) = \frac{\alpha}{2} \left((v_i(t) - y(t))(\text{sign}(v_i(t) - y(t)) + 1) + y(t)(\text{sign}(v_i(t) - y(t)) - 1) \right), \quad (4)$$

where $\alpha = \frac{1}{RC}$.

To introduce a degree of adaptability into the system, we propose a modification of the peak detector model (4), outlined as follows:

$$\dot{y}(t) = \frac{\alpha_1}{2} (v_i(t) - y(t))(\text{sign}(v_i(t) - y(t)) + 1) + \frac{\alpha_2}{2} y(t)(\text{sign}(v_i(t) - y(t)) - 1), \quad (5)$$

where the parameter α in (4) is decomposed into two design parameters α_1 and α_2 . Numerical simulations are conducted to validate our proposed peak detector system. To demonstrate the robustness of our approach, we subject the system to various classes of

external disturbances. For instance, refer to Figure 5, which illustrates the input signal $v_i(t)$ and the peak detector signal $y(t)$, as described in (5). Based on these simulations, it can be inferred that the parameters α_1 and α_2 govern the memory dynamics of $y(t)$. When α_1 is significantly smaller than α_2 , as observed in Figure 5a,d,g, the peak value is not reached. Conversely, in Figure 5b,e,h, the peak value is achieved, but the response behaves slowly and does not precisely align the input but the dynamics of $v(t)$ is remembered. Finally, in Figure 5c,f,i, we obtain the non-modified system. The main idea of the asymmetric peak detector system is to activate the control when a peak value is detected, or almost detected, as desired.

Hence, by tuning adequately the values of parameters α_1 and α_2 , we can modulate different outputs, capturing the input desired values. The asymmetry comes from the decoupled parameter, allowing us to detect a desired value.

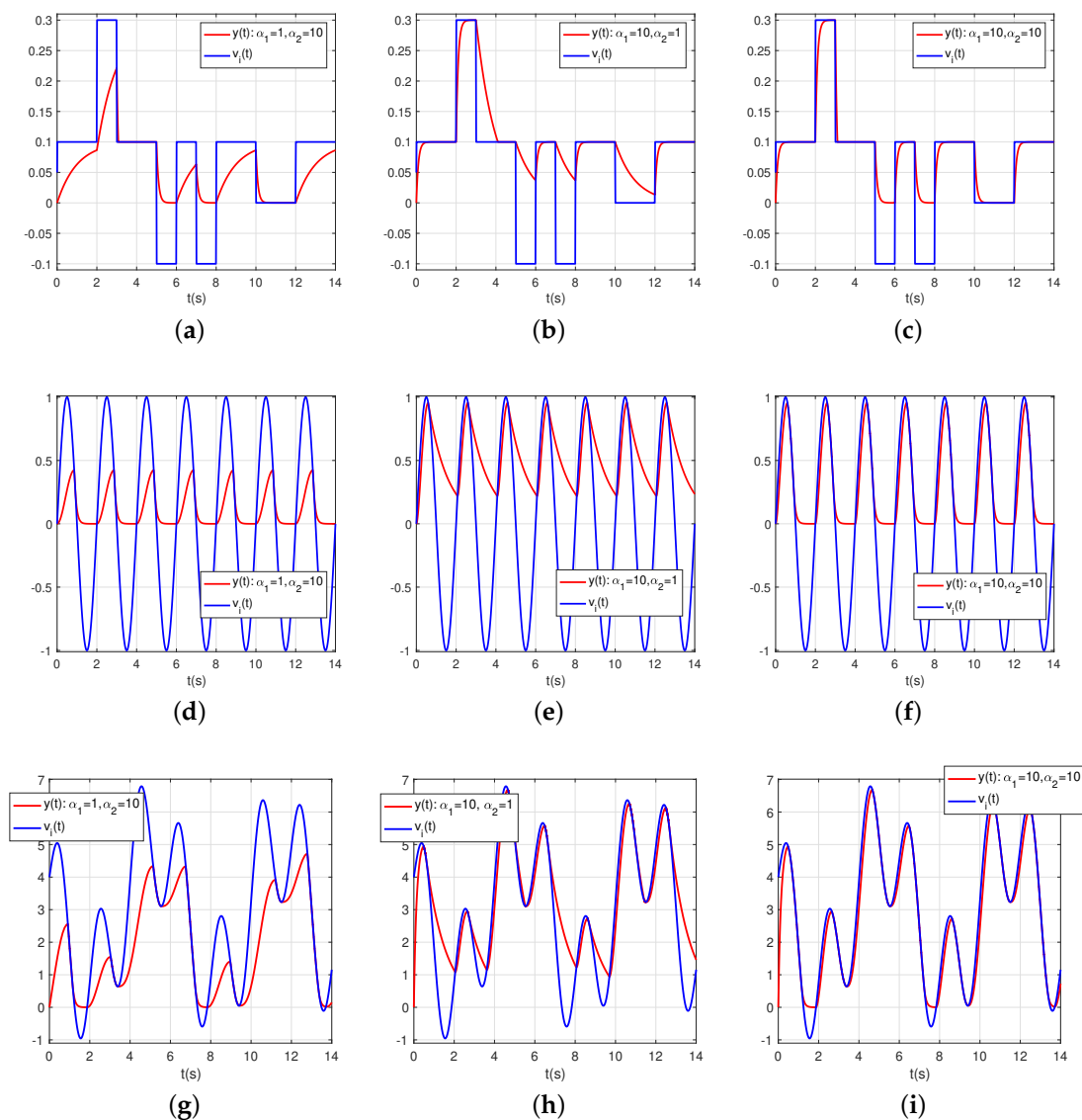


Figure 5. Simulation results of the asymmetric peak detector system (5), when different classes of input $v_i(t)$ are considered; in blue: input $v_i(t)$; in red: output $y(t)$. Three cases of parameters α_1 and α_2 values in (5) are considered for each input function, to expose the performance of the proposal. We obtain a positive response, with different input values detected. The designer needs to determine the preferred scenario for their system.

2.2.2. Bounded-Input Bounded-Output Analysis

According to Figure 5, it appears that our system is Bounded-Input Bounded-Output (BIBO)-stable; if the system input is bounded, that is, if there exists $K > 0$ such that $|v_i(t)| \leq K$, then $y(t)$ is bounded [36]. Let us prove this mathematical hypothesis. Observe that system (5) is equivalent to:

$$\dot{y}(t) = \begin{cases} \alpha_1(v_i(t) - y(t)) & \text{if } v_i(t) \geq y(t) \\ -\alpha_2 y(t) & \text{if } v_i(t) < y(t) \end{cases} \quad (6)$$

By solving the corresponding ordinary differential Equation (6), we obtain:

- If $v_i(t) \geq y(t)$, then $|y(t)| \leq |v_i(t)| \leq K$. In fact, we can obtain:

$$|y(t)| \leq Ke^{-\alpha_1 t_0}.$$

- If $v_i(t) < y(t)$, then $|y(t)| \leq |y_0|e^{-\alpha_2(t-t_0)}$, for $t \geq t_0$ with $y(t_0) = y_0$.

Therefore, the system is exponentially stable, and a Lyapunov function $V_a(t)$ can be stated.

Note that considering $\alpha_1 \gg \alpha_2$, there exists t_0 such that $|y(t)| \leq K|y_0|e^{-\alpha_2(t-t_0)}$, for all $t \geq t_0$.

2.3. Asymmetric Peak Detector Boundary Controller

First, let us introduce the boundary damper controller, previously employed for the vibration control of a cable–tip–mass cable mechanism (refer, for instance, to [23,33,34]):

$$f_d(t) = -k_d u_t(L, t), \quad (7)$$

where $k_d > 0$ is the control gain defined by the designer, and $u_t(L, t)$ is the corresponding feedback signal. The performance of the previous boundary damper controller is comparable, for instance, to the one based on model reference technique design [23]. So, the standard boundary control input in (3) is $f(t) = f_d(t)$.

In our design, the controller $f(t)$ in (3) is constructed, modifying this standard controller $f_d(t)$, as follows. The signal $f_d(t)$ generated by (7) is supplied to our peak detector algorithm (6), i.e., $v_i(t) = f_d(t)$. Then, we define the asymmetric peak detector controller as $f(t) = y(t)$, to be supplied to our cable–tip–mass system (1)–(3). The mathematical model of the asymmetric peak detector controller is then:

$$\dot{y}(t) = \begin{cases} \alpha_1(f_d(t) - y(t)) & \text{if } f_d(t) \geq y(t) \\ -\alpha_2 y(t) & \text{if } f_d(t) < y(t) \end{cases} \quad (8)$$

where α_1 and α_2 are positive constant parameters, and $f_d(t)$ is its input signal. The response $y(t)$ is piecewise continuous and it is available for a given boundary damper controller. Moreover, as said in Section 2.2.2, for any piecewise continuous and bounded signal $f_d(t)$, $y(t)$ is bounded, with $\alpha_1 \gg \alpha_2$. Indeed, there exists a Lyapunov function $V_a(t) = V_a(y(t))$ such that $\dot{V}_a(t) \leq 0$. Hence, we can state the following stability statement:

The closed-loop system (1)–(3) with control input $f(t) = y(t)$ defined in (7) and (8), and with $\alpha_1 \gg \alpha_2$, is BIBO-stable.

The proof is as follows. Consider the following energy-kinetic-like Lyapunov function ([23,33] but the last term):

$$V(t) = \frac{1}{2}\rho \int_0^L u_t^2(x, t)dx + \frac{1}{2}T_0 \int_0^L u_x^2(x, t)dx + \frac{1}{2}mu_t^2(L, t) + V_a(t). \quad (9)$$

Then, it is straightforward to obtain (for simplicity, in some functions, their arguments are intentionally omitted):

$$\dot{V}(t) = \rho \int_0^L u_t u_{tt} dx + T_o \int_0^L u_x u_{xt} dx + m u_t(L, t) u_{tt}(L, t) + \dot{V}_a(t). \tag{10}$$

Taking into account that $\dot{V}_a \leq 0$, by invoking (1) and (3), we have:

$$\dot{V}(t) \leq T_o \int_0^L u_t u_{xx} dx + T_o \int_0^L u_x du_t + u_t(L, t) [-T_o u_x(L, t) + f(t)]. \tag{11}$$

Then, after employing integration by parts and some algebraic simplifications, we arrive to

$$\dot{V}(t) \leq y(t) u_t(L, t). \tag{12}$$

From (8), we have to consider two cases:

- (a) If $f_d(t) \geq y(t)$, then $\dot{V}(t) \leq -k_d u_t(L, t) u_t(L, t) = -k_d u_t^2(L, t) \leq 0$.
- (b) If $f_d(t) < y(t)$, then $-y(t) < -f_d(t)$. Moreover, from (7) we induce that $u_t(L, t) = -\frac{1}{k_d} f_d(t)$. So, $\dot{V}(t) \leq y(t) u_t(L, t) = -y(t) \frac{1}{k_d} f_d(t) < -\frac{1}{k_d} f_d^2(t) \leq 0$.

We can affirm that $\dot{V}(t) \leq 0$, which means that $V(t)$ is bounded, thus concluding our main proof.

We are using the fact that, in real physical systems, if the energy of the systems is bounded, then all surrounding dynamic signals of the closed-loop system are bounded too [23].

3. Results

To analyze the proposed controller design of $f(t)$ as applied to the cable–tip–mass (1)–(3), we prepare two control cases for comparison:

- (i) Standard boundary controller: $f(t) = f_d(t)$ (7);
- (ii) Asymmetric peak detector controller: $f(t) = y(t)$ (7)–(8).

We set the following data: $m = 1$ Kg, $T_o = 1$ N, $\rho = 0.25$ kg/m, and $L = 1$ m. As initial conditions, we impose $u(x, 0) = 0.01 \sin(\pi x)$ and $u_t(x, 0) = 0$. The time interval is $[0, 120]$ s. The value of the control gain k_d will be discussed in the next section. In programming, we use the numerical difference method with $dx = 0.1$ m and $dt = 0.005$ s. This discretization time was also employed for our peak detector system. To evaluate the total system energy employed by the controller, we consider the following functional energy index:

$$E(f) = \frac{1}{T} \int_0^T |f(t)| dt. \tag{13}$$

The current objective in control design is to determine the design parameters α_1 and α_2 with the aim of reducing, if possible, this performance index (13). To conclude the study, we consider the non-perturbed and externally perturbed systems in the following two sections.

3.1. Unperturbed Case Experiments

Consider the system defined in (1)–(3). The asymmetric peak detector parameters are set as $\alpha_1 = 1000$ and $\alpha_2 = 100$, verifying the BIBO constraint. First, we will discuss the controller behavior in the function of the value of the control gain k_d . We consider the case when $k_d = 100$ in (7). In this scenario, the conventional boundary controller exhibits instability. Conversely, the asymmetric peak detector boundary controller demonstrates strong performance, showcasing BIBO stability. Figure 6 depicts the performance of our proposed approach, displaying notable vibration attenuation, in contrast to the instability exhibited by the standard controller, as illustrated in Figure 7. For this experiment, we obtain that the energy index (13) for the proposed controller is $E(y) = 74.9$, in front of the

boundary control energy value of $E(f_d) = 3432.6$.

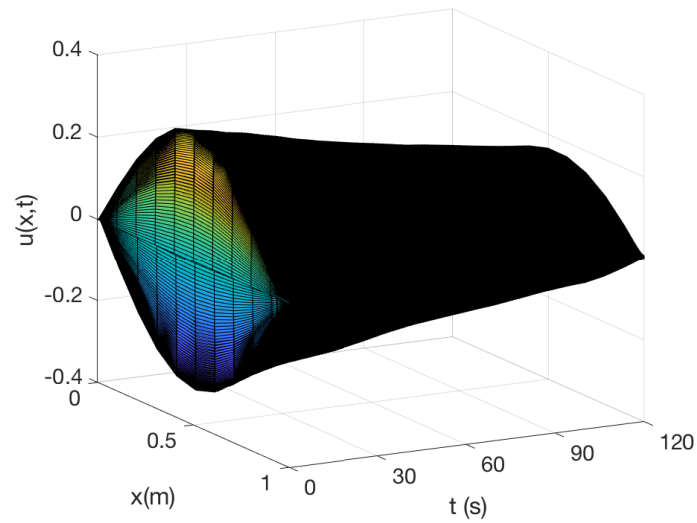


Figure 6. Simulation results for time interval $[0, 120]$, by using the asymmetric peak detector controller (7) and (8), with $k_d = 100$, $\alpha_1 = 1000$ and $\alpha_2 = 100$. The control objective is reached; the vibration decreases.

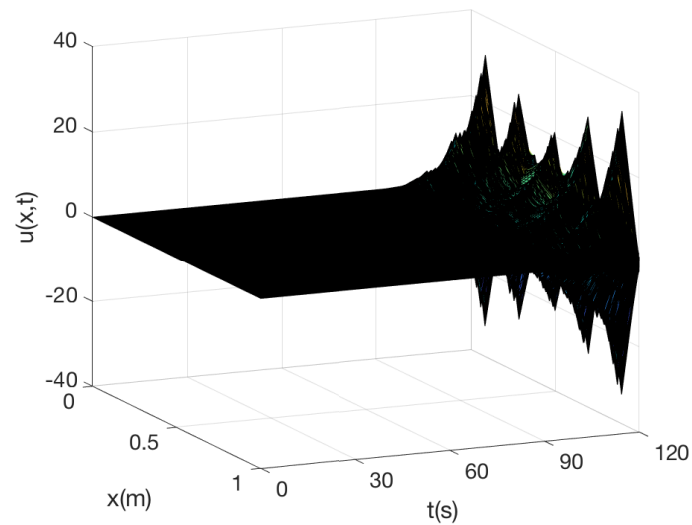


Figure 7. Simulation results for time interval $[0, 120]$, by using the standard boundary damper controller (7), with $k_d = 100$. In contrast to Figure 6, the vibration here does not exhibit bounded behavior.

One alternative for enhancing our performance is to raise the value of the control gain. We set now $k_d = 1000$ (7). The obtained results are shown in Figures 8–11. Using the asymmetric peak detector boundary controller, we induce from Figures 8 and 9 that in twenty seconds, the cable vibration is almost dissipated. On the other hand, under the standard boundary controller, we need fifty seconds to reach similar performance, as illustrated in Figures 10 and 11. We can observe that both controllers spend similar functional energy: $E(y) = 49.0$ and $E(f_d) = 43.3$. Finally, to exemplify the advantage of our asymmetric model, we now consider the symmetric case by setting $\alpha_1 = \alpha_2 = 100$ in (8). These values were tuned online, and the simulation result is presented in Figure 12. It can be inferred that the asymmetric model should be considered.

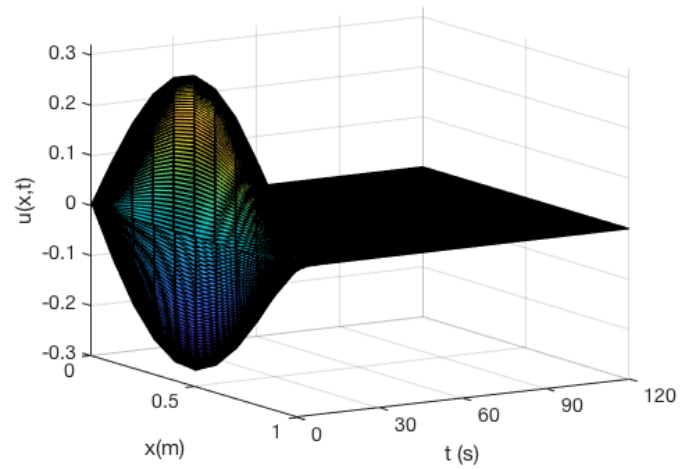


Figure 8. Simulation results of $u(x,t)$ by using the asymmetric peak detector controller (7) and (8), with $k_d = 1000$, $\alpha_1 = 1000$ and $\alpha_2 = 100$.

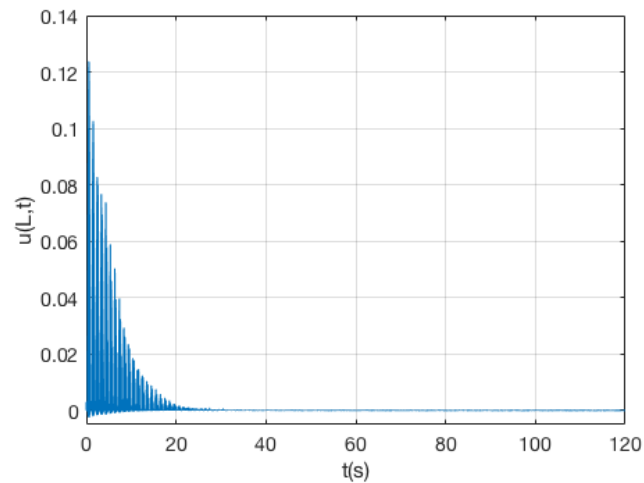


Figure 9. Simulation of $u(L,t)$ versus t , to appreciate the vibration attenuation time of twenty seconds, when the asymmetric peak detector controller (7) and (8) is considered. The rapid response of our controller is attributed to its consideration of peak values.

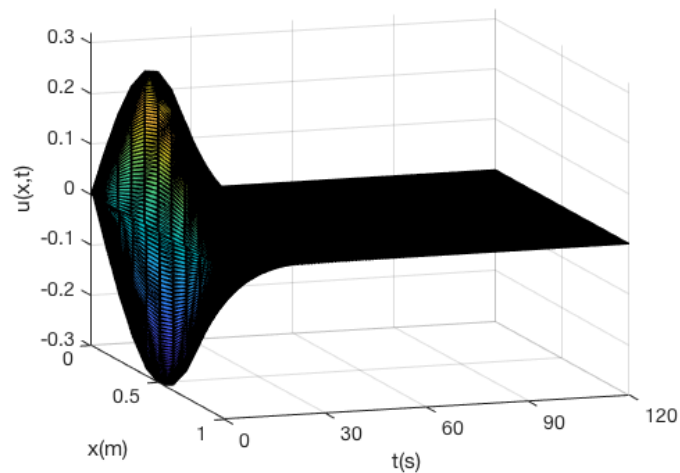


Figure 10. Simulation results $u(x,t)$ by using the standard boundary damper (7), with $k_d = 1000$.

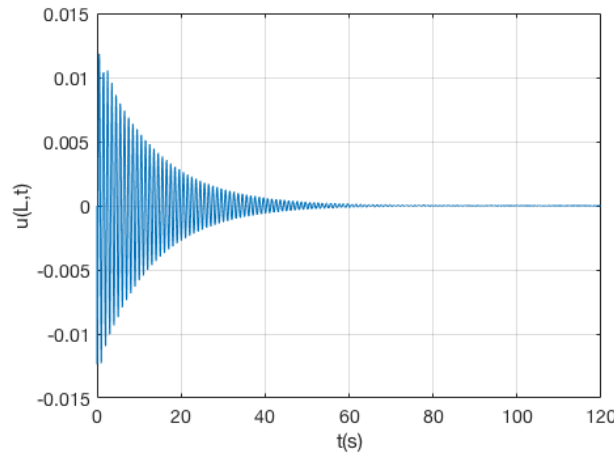


Figure 11. Numerical result of $u(L,t)$ versus t , by using the standard boundary damper (7). The vibration attenuation is reached in fifty seconds.

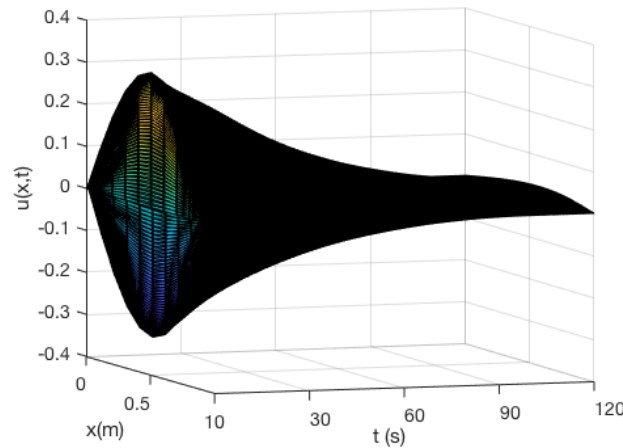


Figure 12. Numerical experiment using the standard peak detector controller (7) and (8), with $\alpha_1 = \alpha_2 = 100$, and control gain $k_d = 1000$.

3.2. External Disturbance Case Experiments

To evaluate the performance of the asymmetric peak detector controller, we examine the realistic case by considering external disturbances affecting the cable. These perturbations are represented by $g(x,t)$ as the disturbance along the cable, and $d(t)$ as the perturbation on the related boundary condition. The system equations are then:

$$\rho u_{tt}(x,t) - T_0 u_{xx}(x,t) = g(x,t), \tag{14}$$

$$u(0,t) = 0, \quad t \geq 0, \tag{15}$$

$$m u_{tt}(L,t) + T_0 u_x(L,t) = f(t) + d(t), \tag{16}$$

$$t \geq 0.$$

The corresponding results are presented in Figures 13–16, from which we deduce that both controllers exhibit similar performance, yet our proposal notably reduces the transient behavior time. The following specific cases are examined. The first case solely considers boundary disturbances:

$$g(x,t) = 0, \quad d(t) = 0.1 + 0.001 \sin(0.2t). \tag{17}$$

Figures 13–15 illustrate the results. We observe that the asymmetric peak detector controller diminishes the time response, even though the total energy (13) is higher for

the peak detector control: $E(y) = 64.51$ versus $E(f_d) = 58.15$. The thickness band of 0.1 shown in Figure 14 is due to the definition of $d(t)$ (17), where the term 0.1 is considered as a boundary condition. The cable inclination is illustrated in Figures 13 and 15.

The second case involves considering only external perturbations along the cable:

$$g(x, t) = 0.001 \cos(\pi x t), \quad d(t) = 0. \tag{18}$$

This disturbance $g(x, t)$ is taken as a reference input, so the cable tries to maintain this shape, as can be observed in Figure 16. In this case, the compared behavior is very similar; the total energy is greater for our proposal ($E(y) = 132.16, E(f_d) = 99.73$), but again the time response is reduced.

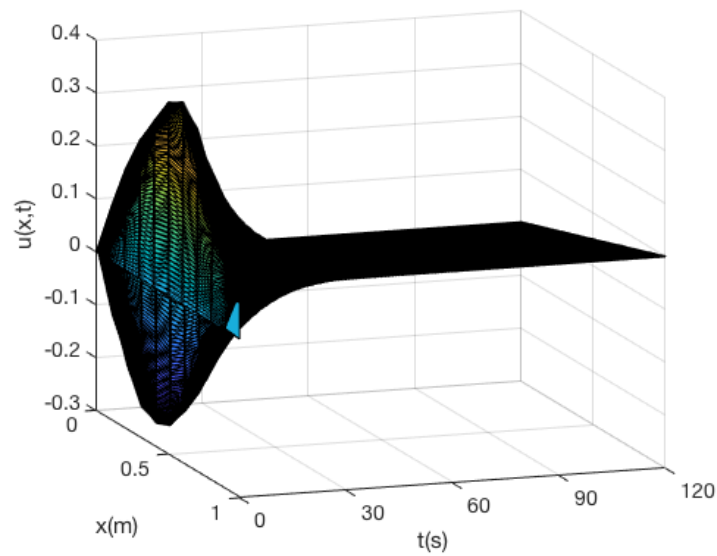


Figure 13. Simulation results by using the standard boundary controller (7), with $k_d = 1000$, of the boundary perturbed system: $g(x, t) = 0$ and $d(t)$ in (17).

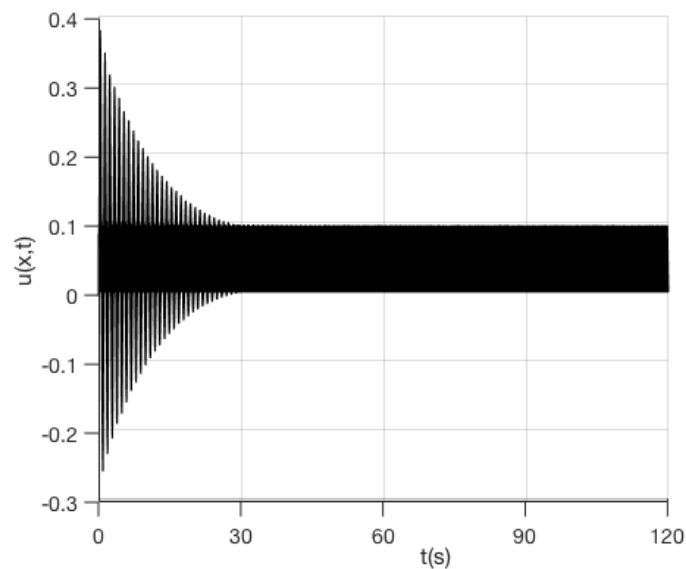


Figure 14. View of the plane $u(x, t)$ versus t (perspective of Figure 13). The thickness band of 0.1 is due to $d(t)$ (17).

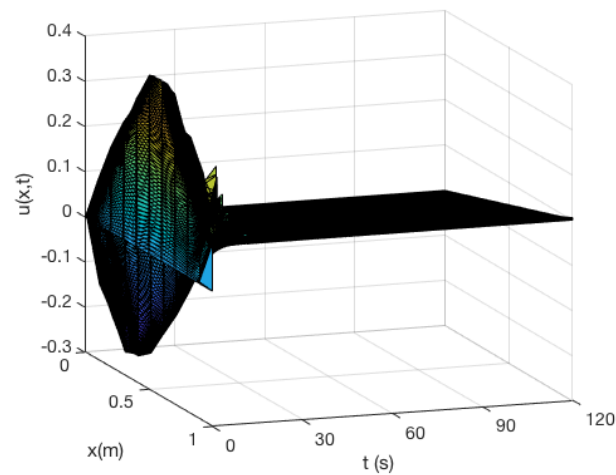


Figure 15. Simulation results by using our design (7) and (8), with $k_d = 1000$, when $g(x, t) = 0$ and $d(t)$ in (17).

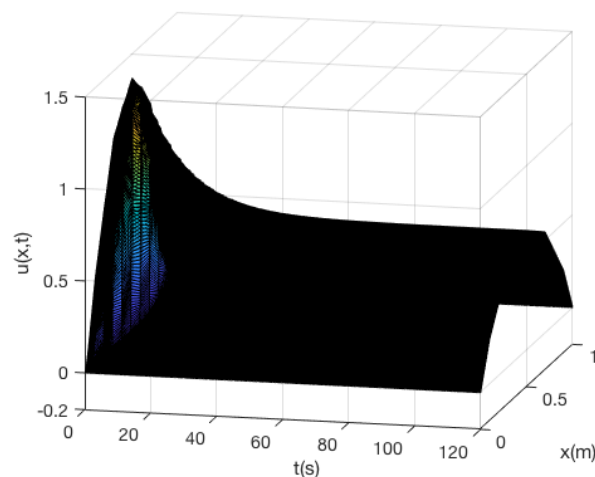


Figure 16. Simulation results by using (8), with $k_d = 1000$, when only disturbance along the cable is considered: $g(x, t)$ in (18) and $d(t) = 0$. This external perturbation $g(x, t)$ is taken as a reference input, so the cable tries to maintain this shape, as can be observed.

The inclusion of the asymmetric peak detector modification in the controller generally enhances the overall performance of the control design, which might specifically manifest as an improvement in the system's response time.

4. Discussion

The present study unveils a modified adaptation of a conventional boundary controller, devised to facilitate a more prompt response while minimizing energy usage in the management of vibrations in a cable–tip–mass system. This innovative approach involves a strategic modification of the peak detector system, incorporating the decoupling of a key design parameter to introduce what we have termed the asymmetric peak detector boundary control. The comparative analysis of its efficacy with the standard boundary damper forms a pivotal aspect of this investigation. Based on these simulations, it can be inferred that the parameters α_1 and α_2 govern the memory dynamics of the system. Hence, by tuning adequately the values of peak detector parameters, we can modulate different outputs, capturing the desired input values. The asymmetry comes from the decoupled parameter, allowing us to detect a desired value.

The results of numerical experiments highlight the effectiveness of the asymmetric peak detector controller in effectively reducing cable vibration, while operating with significantly reduced energy consumption. This successful mitigation not only prevents potential mechanical damage, a common concern associated with the use of unmodified controllers, but also underscores the substantial efficiency improvements brought about by this novel control strategy. When external perturbations are present, our approach may not reduce the total energy, but it significantly reduces the rise time, indicating a noticeable improvement.

Furthermore, the study highlights the moderate increase in total energy consumption when aiming for a swifter system response. These findings serve to emphasize the notable potential of integrating the asymmetric peak detector modification into the controller, thus offering a promising avenue for augmenting the overall efficacy of the control design.

5. Conclusions

In this paper, we introduce a novel modification of a standard boundary controller aimed at achieving a faster response with reduced energy consumption for controlling the vibration of a cable–tip–mass system. To achieve this, we alter the peak detector system by decoupling a design parameter, defining it as the asymmetric peak detector boundary control. Its performance is compared with the standard boundary damper. Numerical experiments indicate that the asymmetric peak detector controller effectively mitigates cable vibration with lower energy consumption, preventing mechanical damage that may arise with the unmodified controller. Additionally, when a faster response is desired, the total energy increase is moderate. The simulations presented in this study suggest that incorporating the asymmetric peak detector modification into the controller can significantly enhance the performance of the control design.

Author Contributions: Conceptualization, L.A. and G.P.-V.; methodology, L.A. and G.P.-V.; software, L.A. and G.P.-V.; validation, G.P.-V.; formal analysis, L.A. and G.P.-V.; investigation, L.A. and G.P.-V.; writing—original draft preparation, L.A. and G.P.-V.; writing—review and editing, L.A. and G.P.-V.; funding acquisition, G.P.-V. All authors have read and agreed to the published version of the manuscript.

Funding: This work has been funded by the Generalitat de Catalunya through the research projects 2021-SGR-01044.

Informed Consent Statement: Not applicable.

Data Availability Statement: No new data were created.

Conflicts of Interest: The authors declare no conflict of interest.

Abbreviations

The following abbreviations are used in this manuscript:

PDE	Partial Differential Equation
BIBO	Bounded-Input Bounded-Output
D	Diode
C	Capacitor
R	Resistor

References

1. Morris, K. *Control of Systems Governed by Partial Differential Equations*; The IEEE Control Theory Handbook; CRC Press: Boca Raton, FL, USA, 2010.
2. Lasieka, I.; Triggiani, R. *Control Theory for Partial Differential Equations: Continuous and Approximation Theories*; Cambridge University Press: Cambridge, UK, 2000.
3. Lagnese, J. *Boundary Stabilization of Thin Plates*; SIAM: Philadelphia, PA, USA, 1989.
4. Bensoussan, A.; Prato, G.D.; Delfour, M.; Mitter, S. *Representation and Control of Infinite-Dimensional Systems*; Birkhauser: Basel, Switzerland, 2006.

5. Acho, L.; Pujol-Vazquez, G. A boundary control technique to the string-tip-mass system based on a non-symmetric peak-detector model. In Proceedings of the International Conference on System Theory, Control and Computing, Sinaia, Romania, 19–21 October 2017; pp. 759–762.
6. Krstic, M.; Smyshlyaev, A. *Boundary Control of PDEs: A Course on Backstepping Designs*; SIAM: Philadelphia, PA, USA, 2008.
7. Luo, N.; Vidal, Y.; Acho, L. *Wind Turbine Control and Monitoring*; Springer: Berlin/Heidelberg, Germany, 2014.
8. Dibaj, A.; Gao, Z.; Nejad, A.R. Fault detection of offshore wind turbine drivetrains in different environmental conditions through optimal selection of vibration measurements. *Renew. Energy* **2023**, *203*, 161–176. [[CrossRef](#)]
9. d’Andréa Novel, B.; Coron, J.M. Exponential stabilization of an overhead crane with flexible cable via a back-stepping approach. *Automatica* **2000**, *36*, 587–593. [[CrossRef](#)]
10. Ballaben, J.S.; Sampaio, R.; Rosales, M.B. Stochastic dynamics of a non-linear cable-beam system. *J. Braz. Soc. Mech. Sci. Eng.* **2016**, *38*, 307–316. [[CrossRef](#)]
11. Caverly, R.J.; Forbes, J.R.; Mohammadshahi, D. Dynamic modeling and passivity-based control of a single degree of freedom cable-actuated system. *IEEE Trans. Control. Syst. Technol.* **2015**, *23*, 898–909. [[CrossRef](#)]
12. Qu, Z. An iterative learning algorithm for boundary control of a stretched string on a moving transporter. In Proceedings of the 3rd Asian Control Conference, Shanghai, China, 4–7 July 2000.
13. Bekiaris-Liberis, N.; Krstic, M. Compensation of wave actuator dynamics for nonlinear systems. *IEEE Trans. Autom. Control* **2014**, *59*, 1555–1570. [[CrossRef](#)]
14. Morgul, O.; Rao, B.P.; Conrad, F. On the stabilization of a cable with a tip mass. *IEEE Trans. Autom. Control* **1994**, *39*, 2140–2145. [[CrossRef](#)]
15. Guo, B.Z. Riesz basis approach to the stabilization of a flexible beam with a tip mass. *SIAM J. Control Optim.* **2001**, *39*, 1736–1747. [[CrossRef](#)]
16. Baicu, C.; Rahn, C.; Nibali, B. Active boundary control of elastic cables: Theory and experiment. *J. Sound Vib.* **1996**, *198*, 17–26. [[CrossRef](#)]
17. Zhang, F.; Dawson, D.; Nagarkatti, S.; Rahn, C. Boundary control for a general class of non-linear string-actuator systems. *J. Sound Vib.* **2000**, *229*, 113–132. [[CrossRef](#)]
18. He, W.; Zhang, S.; Ge, S.S. Adaptive control of a flexible crane system with the boundary output constraint. *IEEE Trans. Ind. Electron.* **2014**, *61*, 4126–4133. [[CrossRef](#)]
19. Li, Y.; Aron, D.; Rahn, C.D. Adaptive vibration isolation for axially moving strings: Theory and experiment. *Automatica* **2002**, *38*, 379–390. [[CrossRef](#)]
20. Shahruz, S. Boundary control of a nonlinear axially moving string. *Int. J. Robust Nonlinear Control* **2000**, *10*, 17–25. [[CrossRef](#)]
21. Zhao, Z.; Liu, Y.; Luo, F. Boundary Control for a Vibrating String System with Bounded Input. *Asian J. Control* **2018**, *20*, 323–331. [[CrossRef](#)]
22. Neusser, Z.; Martin, N.; Pelikán, J.; Pawlik, V.; Beneš, P.; Jan, Z.; Volech, J.; Halamka, V.; Machálka, M.; Valasek, M.; et al. Active vibration damping for manufacturing machines using additional cable mechanisms: Conceptual design. *Int. J. Adv. Manuf. Technol.* **2022**, *122*, 3769–3787. [[CrossRef](#)]
23. De Queiroz, M.S.; Dawson, D.M.; Nagarkatti, S.P.; Zhang, F. *Lyapunov-Based Control of Mechanical Systems*; Springer Science & Business Media: Berlin/Heidelberg, Germany, 2012.
24. Do, K. Stochastic boundary control design for extensible marine risers in three dimensional space. *Automatica* **2017**, *77*, 184–197. [[CrossRef](#)]
25. He, W.; He, X.; Zou, M.; Li, H. PDE Model-based boundary control design for a flexible robotic manipulator with input backlash. *IEEE Trans. Control Syst. Technol.* **2018**, *27*, 790–797. [[CrossRef](#)]
26. Krstic, M.; Guo, B.Z.; Balogh, A.; Smyshlyaev, A. Control of a tip-force destabilized shear beam by observer-based boundary feedback. *J. Control Optim.* **2008**, *47*, 553–574. [[CrossRef](#)]
27. Zhang, S.; He, W.; Li, G. Boundary Control Design for a Flexible System with Input Backlash. In Proceedings of the American Control Conference, Boston, MA, USA, 6–8 July 2016; pp. 6698–6702.
28. Zhang, H.W.; Wang, J.M. Boundary stabilization of an unstable parabolic PDE with a time-varying domain and the external disturbance. *Int. J. Control* **2023**, *1*. [[CrossRef](#)]
29. Kelleche, A.; Saedpanah, F.; Abdallaoui, A. On stabilization of an axially moving string with a tip mass subject to an unbounded disturbance. *Math. Methods Appl. Sci.* **2023**, *46*, 15564–15580. [[CrossRef](#)]
30. Homayounzade, M. Adaptive robust output-feedback boundary control of an unstable parabolic PDE subjected to unknown input disturbance. *Int. J. Syst. Sci.* **2021**, *52*, 2324–2337. [[CrossRef](#)]
31. Pujol-Vázquez, G.; Acho, L. Semi-active control of flexible structures using acceleration information via peak-detector systems. In Proceedings of the 6th World Conference on Structural Control and Monitoring: 6WCSCM. Centre Internacional de Mètodes Numèrics en Enginyeria (CIMNE), Barcelona, Spain, 15–17 July 2014; pp. 1893–1901.
32. Floyd, T. *Electronic Devices*; Prentice-Hall Electronics: Hoboken, NJ, USA, 2005.
33. Cheng, M.B.; Su, W.C. Boundary stabilization and matched disturbance rejection of hyperbolic PDE systems: A sliding-mode approach. In Proceedings of the American Control Conference (ACC), Montreal, QC, Canada, 27–29 June 2012; IEEE: Piscataway, NJ, USA, 2012; pp. 5360–5365.

34. Chen, G. Energy decay estimates and exact boundary-value controllability for the wave-equation in a bounded domain. *J. Mathématiques Pures Appliquées* **1979**, *58*, 249–273.
35. Neusser, Z.; Necas, M.; Pelikán, J.; Karlíček, J.; Pawlik, V.; Benes, P.; Machálka, M.; Sika, Z.; Valásek, M. Mechatronic stiffness of cable-driven mechanisms: A study on production machine model. *Int. J. Adv. Manuf. Technol.* **2022**, *123*, 431–446. [[CrossRef](#)]
36. Ozbay, H. *Introduction to Feedback Control Theory-Chapter 4*; CRC Press: Boca Raton, FL, USA, 2000.

Disclaimer/Publisher’s Note: The statements, opinions and data contained in all publications are solely those of the individual author(s) and contributor(s) and not of MDPI and/or the editor(s). MDPI and/or the editor(s) disclaim responsibility for any injury to people or property resulting from any ideas, methods, instructions or products referred to in the content.